AIP | Review of Scientific Instruments

Progress of beam diagnosis system for EAST neutral beam injector

Y. J. Xu, C. D. Hu, L. Yu, L. Z. Liang, W. T. Zhang, Y. Chen, and X. Li

Citation: Review of Scientific Instruments **87**, 02B934 (2016); doi: 10.1063/1.4936998
View online: http://dx.doi.org/10.1063/1.4936998
View Table of Contents: http://scitation.aip.org/content/aip/journal/rsi/87/2?ver=pdfcov
Published by the AIP Publishing

REVIEW OF SCIENTIFIC INSTRUMENTS **87**, 02B934 (2016)

Progress of beam diagnosis system for EAST neutral beam injector

Y. J. Xu,[a)] C. D. Hu, L. Yu, L. Z. Liang, W. T. Zhang, Y. Chen, and X. Li
Institute of Plasma Physics, Chinese Academy of Sciences, Hefei 230031, China

(Presented 25 August 2015; received 21 August 2015; accepted 20 November 2015; published online 10 December 2015)

Neutral beam injection has been recognized as one of the most effective means for plasma heating. According to the research plan of the EAST physics experiment, two sets of neutral beam injector (NBI) were built and operational in 2014. The paper presents the development of beam diagnosis system for EAST NBI and the latest experiment results obtained on the test-stand and EAST-NBI-1 and 2. The results show that the optimal divergence angle is (0.62°, 1.57°) and the full energy particle is up to 77%. They indicate that EAST NBI work properly and all targets reach or almost reach the design targets. All these lay a solid foundation for the achievement of high quality plasma heating for EAST. © *2015 AIP Publishing LLC.* [http://dx.doi.org/10.1063/1.4936998]

I. INTRODUCTION

Neutral beam injection has been recognized as one of the most effective means for plasma heating.[1–7] According to the research plan of the EAST physics experiment, two sets of neutral beam injector (NBI) (4–8 MW, 10–100 s) were built and operational in 2014.[8,9] In order to ensure NBI system safe and stable operation, a set of reliable beam diagnosis system is essential. This paper introduces the development of beam diagnosis system for EAST NBI and the latest experimental results obtained on the test-stand and EAST-NBI-1 and 2. The results obtained at beam diagnosis system show that EAST NBI operates properly and all targets reach or almost reach the design targets.

II. STRUCTURE OF BEAM DIAGNOSIS SYSTEM

Beam diagnosis system includes water flow calorimeter system, video monitor system, thermocouple system, Doppler shift spectrum (DSS) system, photodiode monitor system, residual gas analyzer, and infrared pyrometer system (shown in Fig. 1).

A. Water flow calorimeter system

Water flow calorimeter system is composed of flow meter, differential temperature transducer, flow switch, pressure switch, and data acquisition system (see Fig. 2). It can measure the flow rate and temperature difference of cooling water for ion source and beamline and calculated the power deposition on the arc chamber, grids, and heat loading components of beamline.[10]

B. Video monitor system

Video monitor system is composed of CCD camera, data transmission optical fiber, and video data server. The CCD camera was installed on the observation window of neutralizer. The video monitor system can obtain the visible light during beam extraction.

C. Thermocouple measurement system

The beams deposit partially as heat load on the materials in the beamline, in order to monitor the temperature, thermocouples are installed in all of heat loading components. Meanwhile, the beam power density distribution and divergence angle can be obtained by calorimeter in which thermocouples are installed according to a certain layout (see Fig. 3).[11]

D. Doppler shift spectrum system

In order to measure the beam species, a set of DSS system has been installed on the EAST NBI. The schematic diagram of the DSS is shown in Fig. 4.[12]

E. Photodiode monitor system

In order to prevent the high energy particle (due to reionization) damaging the drift duct, a set of photodiode monitor system is installed. It is composed of collimator lens, optical fiber, photodiode, and logarithmic amplifier. Photodiode monitor system gathers 656 nm Dα spectral line and converts it to voltage signal, shut down NBI according to the comparing results (see Fig. 5).

F. Inferred pyrometer system

When neutral beam is injected into EAST plasma, a fraction of the beam power passes through the plasma and is deposited on the beam-target tile on the interior walls of the EAST. Inferred pyrometer system can monitor the temperature of tile and shut down NBI when the temperature of tile

Note: Contributed paper, published as part of the Proceedings of the 16th International Conference on Ion Sources, New York, New York, USA, August 2015.

a)Author to whom correspondence should be addressed. Electronic mail: yjxu@ipp.ac.cn

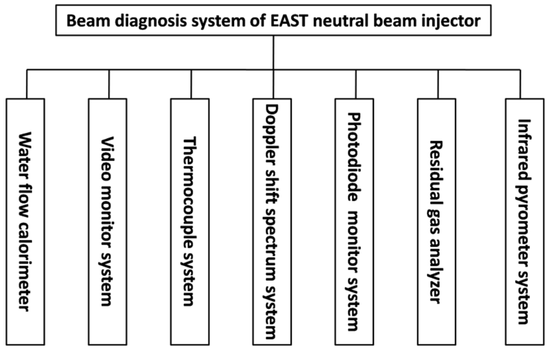

FIG. 1. The block diagram of beam diagnosis system.

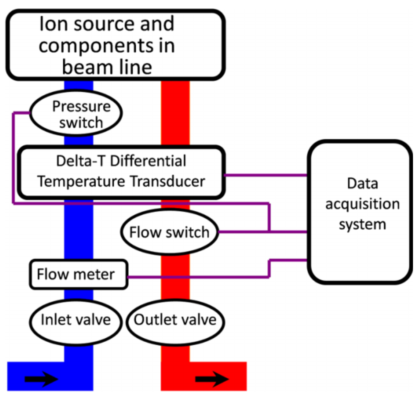

FIG. 2. The diagram of water flow calorimeter system.

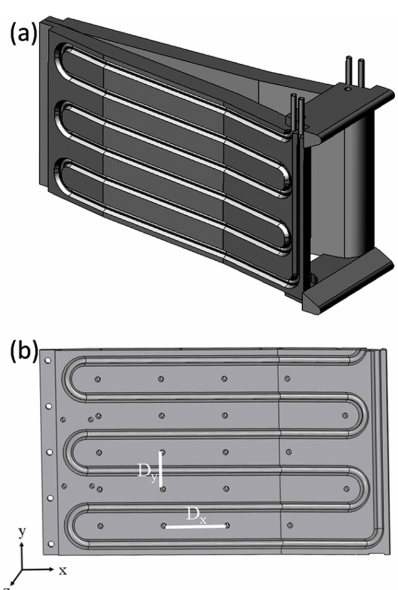

FIG. 3. The structure of the calorimeter (a) three dimensional structures (b) the layout of the thermocouple installed in the plate (Dx = 15.24 cm, Dy = 8.76 cm).

exceeds the setting value. Fig. 6 gives the diagram of inferred pyrometer system.

III. TYPICAL RESULTS AND DISCUSSION

According to data measured from the water flow calorimeter system, the beam power deposition distribution on the heat load components and the power injected into EAST plasma can be obtained (see Fig. 7).

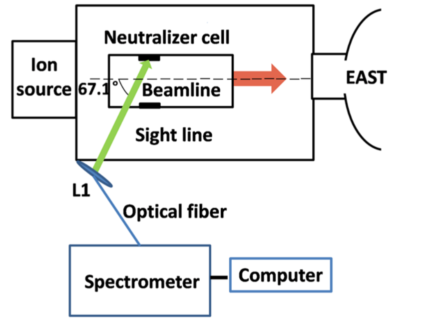

FIG. 4. Schematic diagram of the DSS system.

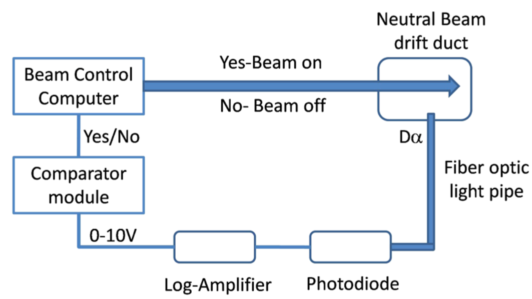

FIG. 5. Block diagram of the photodiode monitor system.

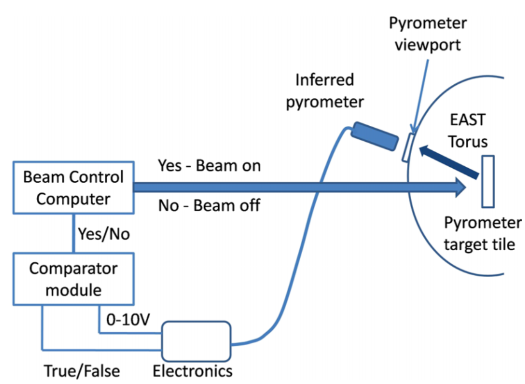

FIG. 6. Block diagram of the inferred pyrometer system.

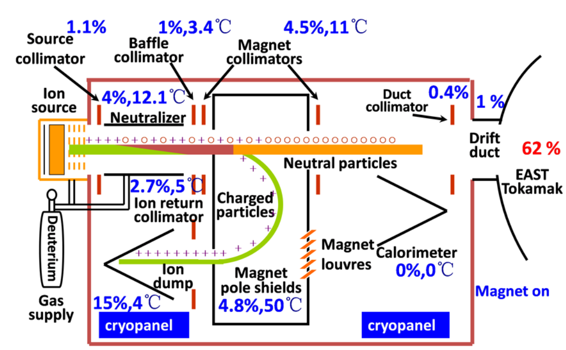

FIG. 7. Beam power distribution on heat load components of beamline (gas flow is 1000 Pa $\cdot$ s^{-1}, Parc = 61 kW, Vacc = 59 kV, Iacc = 32.5 A, τ = 1 s, Pinj = 1.1 MW).

Figure 7 also shows the maximum temperature rise of heat load components. According to the power deposited on

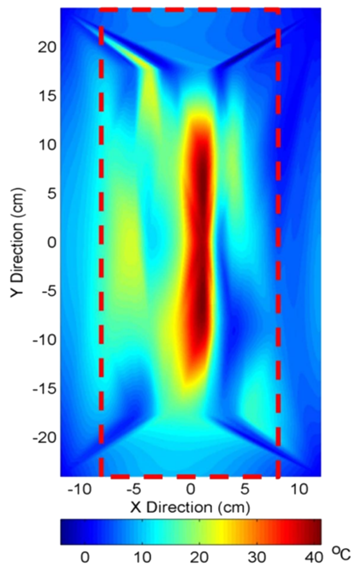

FIG. 8. Distribution of temperature rise on calorimeter (Vacc = 50 kV, Iacc = 32 A, pulse length = 1 s, x-direction: $\alpha = 0.63°$, y-direction: $\beta = 1.57°$).

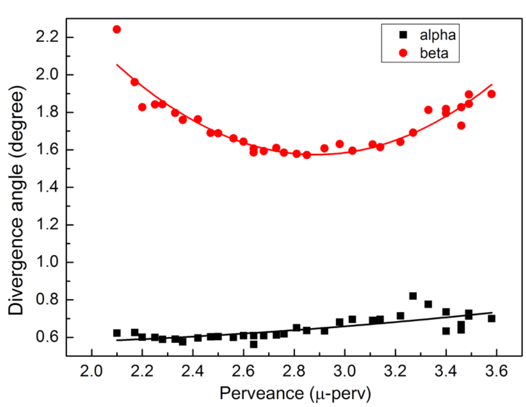

FIG. 9. Divergence angle as a function of perveance (50 keV, beam extraction area: 10 × 48 cm, H-Beam).

the calorimeter with and without the magnetic field of bending magnet, the neutralizing efficiency can be obtained.

The distribution of power density and beam divergence angle is measured using the thermocouples installed in calorimeters. According to the data obtained from the thermocouple, the distribution of temperature rise can be obtained (see Fig. 8). The red dotted bordered rectangle in Fig. 8 corresponds to the entrance of the calorimeter. Figure 8 shows that the beam has a relatively good profile. According to the data obtained from the thermocouple, the divergence angle of x- and y-direction can also be obtained. The relationship between divergence angle and perveance has been shown in Fig. 9.

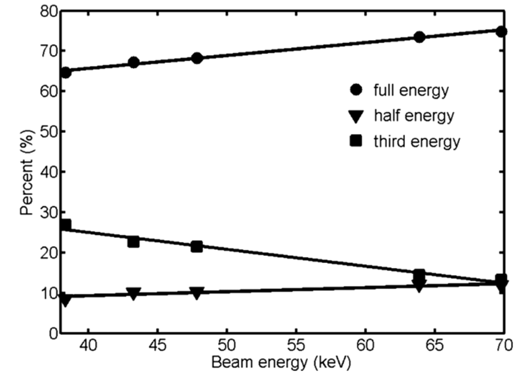

FIG. 10. Beam species as a function of beam energy (for hydrogen).

Beam species is an important parameter for ion source; the relationship between beam species and beam energy is obtained by using DSS system (Fig. 10).

Stable and reliable beam diagnosis system makes it possible for NBI to work properly. The diagnosis results shown above can direct the operation parameter optimization of EAST NBI, in the meantime, the obtaining of key parameters indicates that EAST NBI has an ability of heating plasma.

ACKNOWLEDGMENTS

This work has been supported by the National Magnetic Confinement Fusion Science Program of China (No. 2013GB101001), the International Science and Technology Cooperation Program of China (No. 2014DFG61950), the Presidential Foundation of the Hefei Institutes of Physical Science Chinese Academy of Sciences (Grant No. YZJJ201309), and the Foundation of ASIPP (Contract No. DSJJ-14-JC07).

[1]C. D. Hu and NBI Team, Plasma Sci. Technol. **14**, 567 (2012).
[2]C. D. Hu, L. Z. Liang, Y. L. Xie, J. L. Wet, Y. H. Xie, J. Li, Z. M. Liu, S. Liu, C. C. Jiang, P. Sheng, and Y. J. Xu, Plasma Sci. Technol. **13**, 541 (2011).
[3]C. D. Hu and Y. H. Xie, Plasma Sci. Technol. **14**, 75 (2012).
[4]Y. J. Xu, C. D. Hu, S. Liu, Y. H. Xie, L. Z. Liang, and C. C. Jiang, Chin. Phys. Lett. **29**, 035201 (2012).
[5]Y. H. Xie, C. D. Hu, S. Liu, C. C. Jiang, J. Li, L. Z. Liang, and NBI Team, Rev. Sci. Instrum. **83**, 013301 (2012).
[6]Y. H. Xie, C. D. Hu, S. Liu, L. Z. Liang, Y. J. Xu, Y. L. Xie, C. C. Jiang, P. Sheng, J. Li, and Z. M. Liu, Nucl. Instrum. Methods Phys. Res., Sect. A **727**, 29 (2013).
[7]Y. H. Xie, C. D. Hu, S. Liu, J. Li, and C. C. Jiang, Nucl. Instrum. Methods Phys. Res., Sect. A **676**, 18 (2012).
[8]C. D. Hu, Plasma Sci. Technol. **17**, 1 (2015).
[9]C. D. Hu, Y. J. Xu, Y. L. Xie, S. Liu, Z. M. Liu, P. Sheng, Y. H. Xie, and L. Z. Liang, Chin. Phys. Lett. **32**, 052901 (2015).
[10]L. Yu, C. D. Hu, S. Liu, and Y. J. Xu, J. Fusion Energy **32**, 547 (2013).
[11]L. Yu, C. D. Hu, S. Liu, and Y. J. Xu, J. Fusion Energy **34**, 245 (2015).
[12]L. Z. Liang, Y. Wang, X. X. Zhao, C. D. Hu, S. Liu, Y. H. Xie, C. C. Jiang, Y. J. Xu, Y. L. Xie, and P. Sheng, Phys. Scr. **90**, 045603 (2015).